

中国激光

国产掺镱保偏光纤的制备及其激光性能研究

廖世彪, 罗涛, 肖润珩, 邢颖滨, 褚应波, 彭景刚, 李海清, 李进延, 戴能利*

华中科技大学武汉光电国家研究中心, 湖北 武汉 430074

摘要 基于改进的化学气相沉积(MCVD)工艺,结合溶液掺杂技术,成功制备出 $11 \mu\text{m}/125 \mu\text{m}$ 掺镱保偏光纤,并研究了其激光性能。该光纤的纤芯数值孔径为 0.09,双折射系数值为 3.0×10^{-4} ,915 nm 和 976 nm 处的包层吸收系数分别为 2.48 dB/m 和 7.05 dB/m 。搭建了全光纤振荡器结构测试平台,当掺镱保偏光纤长度为 2.25 m、976 nm 泵浦功率为 57 W 时,实现了最大输出功率为 48.9 W、斜率效率为 85.5% 的激光输出,输出光谱呈洛伦兹型。

关键词 激光光学; 光纤光学; 光纤激光振荡器; 光纤测试; 掺镱保偏光纤

中图分类号 O436

文献标志码 A

DOI: 10.3788/CJL220731

1 引言

光纤激光器因其全固态、高效率、高可靠性、高光束质量等优势而被广泛应用于医疗、通信、国防及工业加工等领域^[1-7]。目前在 $1 \mu\text{m}$ 波段,单链路掺镱连续光纤激光器的激光输出功率已突破 20 kW ^[8],功率的进一步提升存在理论极限^[9]。多数高功率光纤激光器研究集中于随机偏振的掺镱光纤激光器^[10-12]。然而,远距离激光通信、相干探测、高功率光束相干合成等领域的发发展对激光功率、线宽、偏振态等性能的要求越来越高^[13],如何获得高功率、窄线宽、高偏振消光比的光纤激光输出已经成为高功率光纤激光关键领域的研究重点。

其中,高功率、窄线宽线偏振光纤激光器最重要的部分就是提供增益的掺镱保偏光纤,其被应用在种子源以及放大光路中。种子源的性能对整个光纤放大器起决定性作用^[14-15]。2015 年,天津大学基于 $10 \mu\text{m}/125 \mu\text{m}$ 掺镱保偏光纤搭建了一级预放大种子源,实现了 5.6 W 的种子激光输出,最终通过主放大输出了 0.52 kW 的线宽为 30 GHz 的线偏振激光输出^[16]。2020 年,中国工程物理研究院采用 $10 \mu\text{m}/125 \mu\text{m}$ 掺镱保偏光纤搭建了振荡与放大一体化的种子源,输出了 10.68 W 的线偏振种子,线宽为 0.0307 nm ,最终实现了 3.08 kW 的线偏振激光输出^[17]。目前国内线偏振光纤激光器采用的光纤以进口增益保偏光纤居多,在当前大环境下,性能优异的掺镱保偏光纤的国产化势在必行。

本文基于改进的化学气相沉积(MCVD)工艺,结合溶液掺杂技术,成功制备出掺镱保偏光纤。展示了

预制棒折射率的分布规律,搭建了拍长和应力双折射系数的测试系统,进行了保偏特性的测量,并利用消光比测试仪测试了其偏振消光比(PER)。搭建了全光纤振荡器结构测试平台,研究了掺镱保偏光纤激光性能以及线宽性能,实现了最高功率为 48.9 W 、斜率效率为 85.5% 的激光输出。

2 光纤制备、基本参数及保偏特性

2.1 光纤制备与基本参数

本文基于 MCVD 工艺,结合溶液掺杂技术,制备出了 $11 \mu\text{m}/125 \mu\text{m}$ 掺镱保偏光纤(PM-YDF)。利用实验室现有的 MCVD 机床设备,经过腐蚀、沉积、液相掺杂、干燥、玻璃化、塌缩、烧实等过程后制备出预制棒。首先,在高温作用下生成的氧化物附着在石英管内壁,先后形成阻挡层和疏松芯层;接着取下 MCVD 设备上已经沉积有阻挡层和疏松层的石英管,将含有 Yb/Al 离子的水溶液注入到疏松多孔结构的芯层中,并使溶液浸满整个反应管;随后,将完成离子掺杂的反应管进行玻璃化、塌缩和烧实处理。在初步的光纤预制棒形成后,进行直径和剖面的折射率测试,选择合适的套管进行高温加热,以满足芯包比要求。在预制棒的包层区域,沿纤芯对称钻取两个孔,并将掺硼的低折射率石英棒放入孔中。最后,在 1980°C 的温度下,预制棒组件被拉成目标尺寸的光纤,并进行涂敷和紫外固化。

实验制备出的 $11 \mu\text{m}/125 \mu\text{m}$ PM-YDF 如图 1 所示,其中图 1(a)为光纤的显微镜截面图,图 1(b)为预制棒的折射率剖面图。 $11 \mu\text{m}/125 \mu\text{m}$ PM-YDF 的纤芯尺寸为 $11.01 \mu\text{m}$,包层直径为 $125.08 \mu\text{m}$,从左到右

收稿日期: 2022-04-07; 修回日期: 2022-05-16; 录用日期: 2022-06-22; 网络首发日期: 2022-07-02

基金项目: 国家自然科学基金(11875139)

通信作者: *dailn@mail.hust.edu.cn

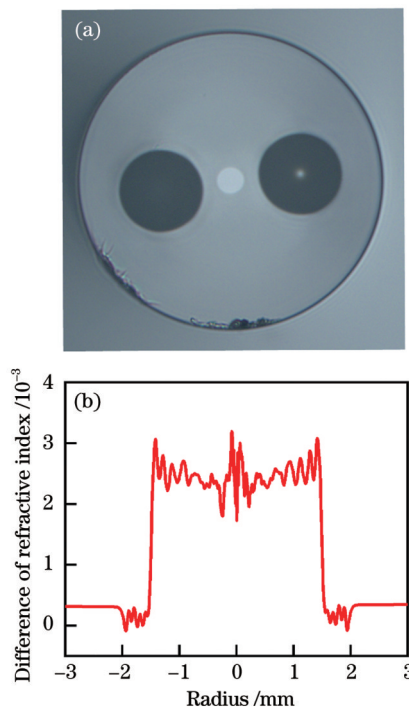


图 1 掺镱保偏光纤。(a) 光纤截面;(b) 折射率剖面

Fig. 1 Ytterbium-doped polarization-maintaining fiber. (a) Optical fiber cross section; (b) refractive index profile

应力区直径依次为 $34.76 \mu\text{m}$ 和 $34.68 \mu\text{m}$ 。保偏光纤中应力区的存在破坏了包层的对称结构,泵浦光不能以螺旋光的形式存在于包层中,从而提升了光纤的包层吸收系数。采用截断法测试了光纤包层的吸收系数, $11 \mu\text{m}/125 \mu\text{m}$ PM-YDF 在 915 nm 处的包层吸收系数为 2.48 dB/m ,在 976 nm 处的包层吸收系数为 7.05 dB/m 。

2.2 双折射系数和保偏特性测试

精确测量保偏光纤的双折射系数对于评估其偏振保持能力具有重要价值,本文采用混合光纤 Sagnac 干涉法^[18]来测量保偏光纤的双折射系数。混合光纤 Sagnac 干涉法的光路图如图 2 所示,除了待测光纤外,其余光学器件都为非保偏的器件,这样可以激起熔接界面处强烈的偏振模反射,待测光纤为本课题组制备出的 $11 \mu\text{m}/125 \mu\text{m}$ PM-YDF。 2×2 耦合器两个臂的分光比均为 $50:50$,且采用的是单模非保偏光纤。宽谱光源产生的信号光通过耦合器后被分为两路并注入到待测光纤中。经过待测光纤后,由于双折射的影

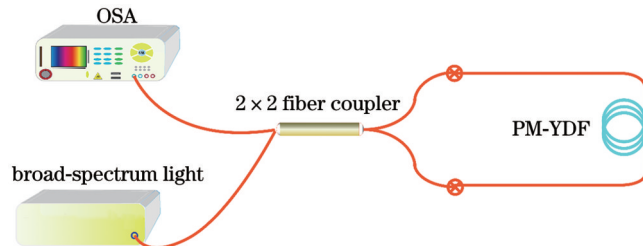


图 2 双折射系数的测试装置图

Fig. 2 Test device diagram of birefringence coefficient

响,两路光产生相应的时延,在耦合器处产生干涉。最终形成的干涉图样可以由耦合器另一端连接的光谱分析仪采集到。所采用的光谱分析仪(OSA)的最小分辨率为 0.02 nm ,满足测量待测光纤光谱干涉周期的需求。

双折射系数(B)和拍长(L_B)的换算关系为

$$L_B = \frac{\lambda}{B}, \quad (1)$$

式中: λ 为光波的中心波长。

当光波在混合光纤 Sagnac 干涉仪中传播时,拍长的表达式为

$$L_B = \frac{\Delta\lambda}{\lambda} L, \quad (2)$$

式中: $\Delta\lambda$ 为光谱仪采集到的干涉图样中的相邻波谷间隔; L 为待测光纤的传播距离。联立式(1)、(2)可以得到保偏光纤双折射系数的表达式:

$$B = \frac{\lambda^2}{\Delta\lambda \cdot L}. \quad (3)$$

光纤的拍长光谱图如图 3 所示,经计算,待测光纤 $11 \mu\text{m}/125 \mu\text{m}$ PM-YDF 的双折射系数值为 3.0×10^{-4} 。为了验证测试系统的准确性,测量了商用光纤(PLMA-YDF-10/125-M)的双折射系数值,其测试值为 3.1×10^{-4} ,与给定的标准值 3.0×10^{-4} 相比,误差率为 3.33% ,在实验允许的误差范围内。同时,利用偏振消光比测试仪对保偏光纤进行了偏振保持能力的实际测量。将消光比为 $>25 \text{ dB}$ 、波长为 1310 nm 的线偏振光通入到长度大于 2.25 m 的 $11 \mu\text{m}/125 \mu\text{m}$ PM-YDF 中, $11 \mu\text{m}/125 \mu\text{m}$ PM-YDF 的另一端被接入到消光比测试仪的接收端口处,消光比测试仪测量的偏振消光比 $>18 \text{ dB}$,证实了本课题组制备的 $11 \mu\text{m}/125 \mu\text{m}$ PM-YDF 满足实际应用的需求。

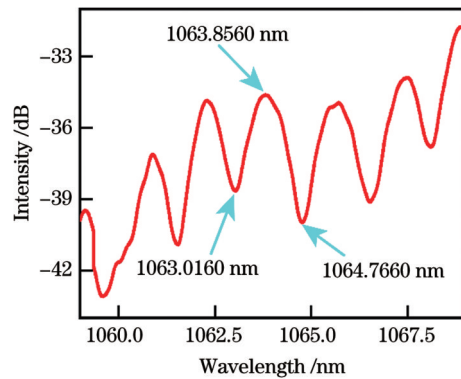


图 3 掺镱保偏光纤的拍长光谱图

Fig. 3 Spectrum of PM-YDF beat length

3 激光性能

3.1 激光实验装置

实验光路如图 4 所示。最前端是一个 976 nm 的

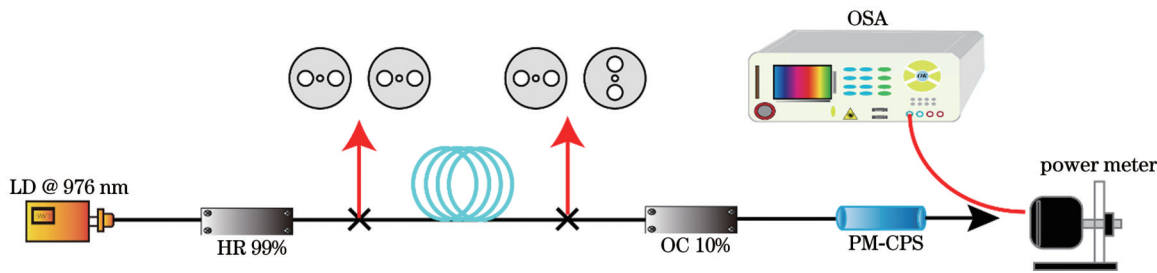


图 4 基于振荡器结构的全保偏光纤激光器结构图

Fig. 4 Structural diagram of all polarization maintaining fiber laser based on oscillator structure

稳波长半导体激光器(LD),与1064 nm的保偏高反光栅(HR 99%)相连接,高反光栅在1064 nm附近的反射率为99%。采用平行熔接的方式将保偏高反光栅与掺镱保偏光纤熔接,需要注意的是,发热情况较严重,一定要保证光纤的洁净程度,避免对整个激光器造成破坏。采用正交熔接的方式将接着掺镱保偏光纤的另一端与保偏低反光栅(OC 10%)熔接,利用保偏光栅偏振模选择的基本原理,从保偏光纤的慢轴输出线偏振激光,使用保偏包层光滤除器(CPS)滤除靠近输出端的包层光。振荡腔中掺镱保偏光纤的长度为2.25 m,采用9 cm的弯曲直径以抑制高阶模的输出,保证激光近单模。同时,由于保偏光纤的快轴偏振模的弯曲损耗大于慢轴偏振模,此弯曲直径也有助于提升输出激光的偏振消光比。输出端光纤切8°斜角以防止寄生振荡,采用量程为200 W的功率计探头对输出激光进行功率记录。所有光纤器件均放置在16 °C

的水冷板上进行散热处理。功率计靶面上的散射光通过多模跳线被收集到光谱仪中进行光谱成分分析。

3.2 实验结果与讨论

实验利用高反保偏光栅的快轴与低反保偏光栅的慢轴进行偏振选模,线偏振激光沿低反保偏光栅的慢轴输出,低反保偏光栅慢轴的反射光谱的半峰全宽为0.06 nm。为了保证相同的吸收,以下实验中有源光纤的长度分别为2.25 m和3.25 m。当有源光纤为11 μm/125 μm PM-YDF时,激光器的输出功率随泵浦功率的变化曲线如图5(a)所示。可以看出:随着泵浦功率的增加,输出功率趋于线性增长,未出现功率抖动;当泵浦功率为57 W时,输出激光功率为48.9 W,此时功率最高,功率进一步增长受限于泵浦功率;线性拟合效率为85.5%。当有源光纤为PLMA-YDF-10/125-M时,其在976 nm处的包层吸收系数为4.95 dB/m,激光器的输出功率随着泵浦功率的变化曲线如图5(b)所示,

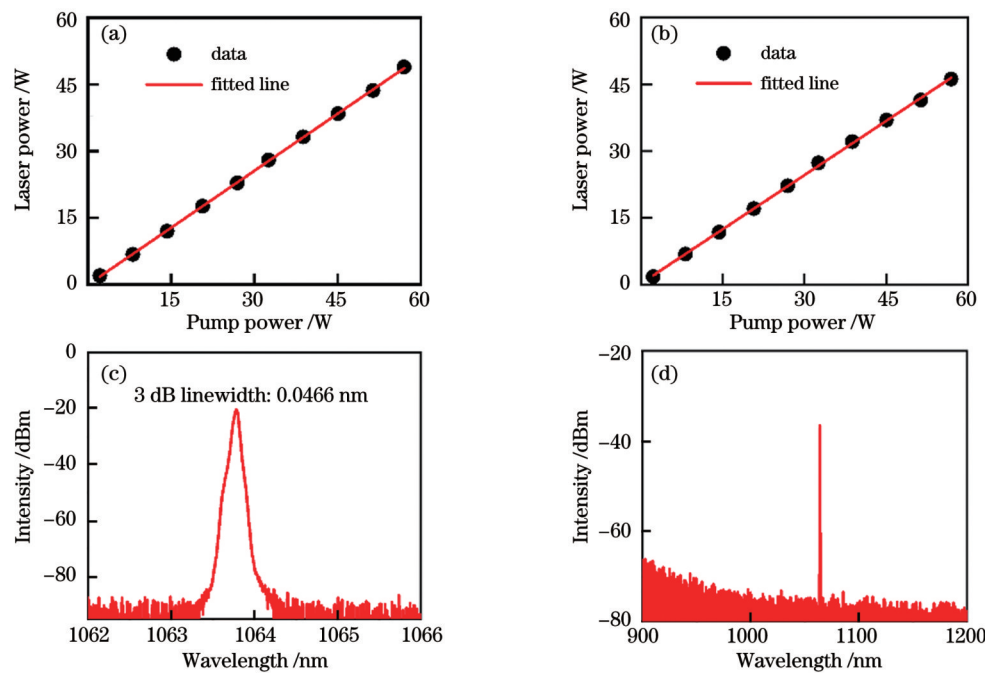


图5 实验结果。(a)11 μm/125 μm PM-YDF的输出功率随泵浦功率的变化曲线;(b)PLMA-YDF-10/125-M的输出功率随泵浦功率的变化曲线;(c)11 μm/125 μm PM-YDF在12 W激光功率下的输出光谱图;(d)11 μm/125 μm PM-YDF在48.9 W激光功率下的输出光谱图

Fig. 5 Experimental results. (a) Output power of 11 μm/125 μm PM-YDF versus pump power; (b) output power of PLMA-YDF-10/125-M versus pump power; (c) output spectrum of 11 μm/125 μm PM-YDF when laser power is 12 W; (d) output spectrum of 11 μm/125 μm PM-YDF when laser power is 48.9 W

输出功率呈线性增长,当泵浦功率为 57 W 时,输出激光功率为 46.2 W,线性拟合效率为 82.7%。可以看出,无论是激光器的最高输出功率还是泵浦光转化为激光的效率,11 μm/125 μm PM-YDF 都表现优异。当使用 11 μm /125 μm PM-YDF 时,光纤激光器在 12 W 激光功率下的输出光谱图如图 5(c)所示,光谱形状呈洛伦兹型,单峰,此时光谱的半峰全宽为 0.0466 nm,基频噪声的抑制效果良好,未出现杂峰。当使用 11 μm /125 μm PM-YDF 时,光纤激光器在最高激光功率 48.9 W 下的光谱图如图 5(d)所示,可以看出,无剩余泵浦光和拉曼信号峰。

4 结 论

采用改进的化学气相沉积工艺,结合溶液掺杂技术,成功制备出国产化的 11 μm/125 μm 掺镱保偏光纤。其双折射系数值为 3.0×10^{-4} ,在 2.25 m 光纤长度下,保持不低于 18 dB 的偏振度。搭建了全光纤振荡器结构测试平台,实现了在 1064 nm 处 48.9 W 的激光输出,斜率效率高达 85.5%,验证了掺镱保偏光纤良好的激光性能。

参 考 文 献

- [1] Richardson D J, Nilsson J, Clarkson W A. High power fiber lasers: current status and future perspectives[J]. Journal of the Optical Society of America B, 2010, 27(11): B63-B92.
- [2] Jauregui C, Limpert J, Tünnermann A. High-power fibre lasers [J]. Nature Photonics, 2013, 7(11): 861-867.
- [3] Fomin V, Gapontsev V, Shecherbakov E, et al. 100 kW CW fiber laser for industrial applications[C]// 2014 International Conference Laser Optics, June 30-July 4, 2014, St. Petersburg, Russia. New York: IEEE Press, 2014.
- [4] Wang Y Y, Gao C, Tang X, et al. 30/900 Yb-doped aluminophosphosilicate fiber presenting 6.85-kW laser output pumped with commercial 976-nm laser diodes[J]. Journal of Lightwave Technology, 2018, 36(16): 3396-3402.
- [5] Quintino L, Costa A, Miranda R, et al. Welding with high power fiber lasers-a preliminary study[J]. Materials & Design, 2007, 28 (4): 1231-1237.
- [6] Kalisky O. The status of high-power lasers and their applications in the battlefield[J]. Optical Engineering, 2010, 49(9): 091003.
- [7] Zervas M N, Codemard C A. High power fiber lasers: a review[J]. IEEE Journal of Selected Topics in Quantum Electronics, 2014, 20(5): 0904123.
- [8] Shiner B. The impact of fiber laser technology on the world wide material processing market[C]// CLEO: Science and Innovations 2013, June 9-14, 2013, San Jose, California, USA. Washington, D.C.: OSA, 2013: AF2J.1.
- [9] Dawson J W, Messerer M J, Beach R J, et al. Analysis of the scalability of diffraction-limited fiber lasers and amplifiers to high average power[J]. Optics Express, 2008, 16(17): 13240-13266.
- [10] 王岩山, 马毅, 彭万敬, 等. 基于近平顶光谱实现 3.6 kW 窄线宽线偏振近单模光纤激光输出 [J]. 中国激光, 2021, 48(23): 2316001.
- [11] Wang Y S, Ma Y, Peng W J, et al. Realization of 3.6 kW narrow linewidth linear polarization near-single mode fiber laser output based on near-flat top spectrum[J]. Chinese Journal of Lasers, 2021, 48(23): 2316001.
- [12] 宋家鑫, 任帅, 王广建, 等. 国产锥形光纤实现 4.2 kW 近单模窄线宽激光[J]. 中国激光, 2022, 49(8): 0816002.
- [13] Song J X, Ren S, Wang G J, et al. Realization of 4.2 kW near-single mode narrow linewidth laser by domestic tapered fiber[J]. Chinese Journal of Lasers, 2022, 49(8): 0816002.
- [14] 马鹏飞, 宋家鑫, 王广建, 等. 高功率窄线宽光纤激光突破 6 kW 级近单模输出[J]. 中国激光, 2022(9): 0916002.
- [15] Ma P F, Song J X, Wang G J, et al. High power narrow linewidth fiber laser breaks through 6 kW near single mode output[J]. Chinese Journal of Lasers, 2022(9): 0916002.
- [16] 马毅, 颜宏, 彭万敬, 等. 基于多路窄线宽光纤激光的 9.6 kW 共孔径光谱合成光源[J]. 中国激光, 2016, 43(9): 0901009.
- [17] Ma Y, Yan H, Peng W J, et al. 9.6 kW common aperture spectral beam combination system based on multi-channel narrow-linewidth fiber lasers[J]. Chinese Journal of Lasers, 2016, 43(9): 0901009.
- [18] Qi Y F, Yang Y F, Shen H, et al. 2.7 kW CW narrow linewidth Yb-doped all-fiber amplifiers for beam combining application[C]// Advanced Solid State Lasers 2017, October 1-5, 2017, Nagoya, Aichi, Japan. Washington, D.C.: OSA, 2017: ATu3A.1.
- [19] Lin H, Tao R, Li C, et al. 3.7 kW monolithic narrow linewidth single mode fiber laser through simultaneously suppressing nonlinear effects and mode instability[J]. Optics Express, 2019, 27(7): 9716-9724.
- [20] Shi W, Fang Q, Fan J L, et al. High power monolithic linearly polarized narrow linewidth single mode fiber laser at 1064 nm[C]// 2015 11th Conference on Lasers and Electro-Optics Pacific Rim (CLEO-PR), August 24-28, 2015, Busan, Korea (South). New York: IEEE Press, 2015.
- [21] Wang Y S, Ke W W, Peng W J, et al. 3 kW, 0.2 nm narrow linewidth linearly polarized all-fiber laser based on a compact MOPA structure[J]. Laser Physics Letters, 2020, 17(7): 075101.
- [22] 徐春娇, 杨远洪, 段伟倩, 等. 基于 Sagnac 干涉仪的保偏光纤拍长测试技术[J]. 北京航空航天大学学报, 2010, 36(6): 753-756.
- [23] Xu C J, Yang Y H, Duan W Q, et al. Technology of measuring the beat-length of polarization maintain optical fiber based on Sagnac interferometer[J]. Journal of Beijing University of Aeronautics and Astronautics, 2010, 36(6): 753-756.

Preparation of Domestic Ytterbium-Doped Polarization-Maintaining Fiber and Study of Its Laser Properties

Liao Shibiao, Luo Tao, Xiao Runheng, Xing Yingbin, Chu Yingbo, Peng Jinggang,
Li Haiqing, Li Jinyan, Dai Nengli*

Wuhan National Laboratory for Optoelectronics, Huazhong University of Science and Technology, Wuhan 430074,
Hubei, China

Abstract

Objective Since the 1990s, fiber lasers have been widely used in the medical, communications, national defense, and industrial processing fields because of their all-solid state, high efficiency, high reliability, and high beam quality. At present, in the $1\text{ }\mu\text{m}$ band, the output power of a single-link ytterbium-doped continuous fiber laser exceeds 20 kW, and there is a theoretical limit to further increases in this power. Most studies on high-power fiber lasers have focused on randomly polarized ytterbium-doped fiber lasers. However, the development of long-distance laser communication, coherent detection, high-power beam coherent synthesis, and other applications has higher requirements for laser power, linewidth, polarization state, and other properties. Obtaining a high-power, narrow-linewidth, and high polarization extinction ratio fiber laser output has become the focus and research direction in the field of high-power fiber lasers. The most important part of a high-power narrow-linewidth linearly polarized fiber laser is the ytterbium-doped polarization-maintaining fiber, which provides gain. In this study, based on a modified chemical vapor deposition (MCVD) process combined with solution doping technology, a ytterbium-doped polarization-maintaining fiber is successfully fabricated. The polarization extinction ratio (PER) is determined by using an extinction ratio tester. An all-fiber oscillator structure test platform is built, and the performance, polarization characteristics, and linewidth performance of the ytterbium-doped polarization-maintaining fiber lasers are studied.

Methods In this study, a $11\text{ }\mu\text{m}/125\text{ }\mu\text{m}$ ytterbium-doped polarization-maintaining fiber (PM-YDF) was fabricated using the MCVD process combined with solution doping technology. Using existing MCVD machine tool equipment in the laboratory, the preform was prepared after etching, deposition, liquid-phase doping, drying, vitrification, collapse, and burning. Two holes were drilled symmetrically along the fiber core in the cladding region of the preform, and a boron-doped low-refractive-index quartz rod was placed in the holes. Finally, at a temperature of $1980\text{ }^\circ\text{C}$, the preform assembly was drawn into a fiber with the target size, coated, and UV-cured. The refractive index profile (RIP) of the fiber was analyzed and the absorption coefficient of the fiber was tested. A birefringence coefficient measurement system was built, and hybrid fiber Sagnac interferometry was used to measure the birefringence coefficient of the polarization-maintaining fibers. An all-fiber oscillator structure test platform was built to evaluate the laser performance of the fiber.

Results and Discussions The experimentally prepared $11\text{ }\mu\text{m}/125\text{ }\mu\text{m}$ PM-YDF is shown in Fig. 1, in which Fig. 1(a) shows the microscope cross-section of the fiber, and Fig. 1(b) shows the refractive index cross-section of the preform. It can be observed that the core ellipticity of the fiber is very low. The optical fiber cladding absorption coefficient is measured by the truncation method, and the cladding absorption coefficients of $11\text{ }\mu\text{m}/125\text{ }\mu\text{m}$ PM-YDF at 915 nm and 976 nm are 2.48 dB/m and 7.05 dB/m , respectively. The spectrum of the fiber beat length is shown in Fig. 3. After calculation, the birefringence coefficient value of the fiber to be tested, $11\text{ }\mu\text{m}/125\text{ }\mu\text{m}$ PM-YDF, is 3.0×10^{-4} , with good performance. Simultaneously, the polarization-maintaining (PM) fiber is measured using a polarization extinction ratio tester. Linearly polarized light with a $\text{PER} > 25\text{ dB}$ and a wavelength of 1310 nm is passed into the $11\text{ }\mu\text{m}/125\text{ }\mu\text{m}$ PM-YDF sample with length of $> 2.25\text{ m}$, and the PER measured by the PER tester is $> 18\text{ dB}$, which confirms that $11\text{ }\mu\text{m}/125\text{ }\mu\text{m}$ PM-YDF can meet the needs of practical applications. An oscillator structure test platform is constructed. When the active fiber is $11\text{ }\mu\text{m}/125\text{ }\mu\text{m}$ PM-YDF, the output power of the laser varies with the pump power, as shown in Fig. 5(a). As the pump power increases, the output power also increases. The power tends to increase linearly, and there is no power jitter. When the pump power is 57 W , the output laser power is 48.9 W , which represents the maximum output power obtained. Further increase in the output power is limited by the pump power, and the linear fitting efficiency is 85.5% . Figure 5(c) shows the output spectrum of the fiber laser with a laser power of 12 W . The spectral shape is the Lorentzian type with a single peak. The full width at half maximum is 0.0466 nm . The frequency noise is well-suppressed, no spurious peaks appear, and the polarization extinction ratio at this power is $> 18\text{ dB}$.

Conclusions A domestically produced $11\text{ }\mu\text{m}/125\text{ }\mu\text{m}$ PM-YDF is successfully fabricated using an MCVD process combined with solution doping technology. It has a birefringence value of 3.0×10^{-4} and maintains a degree of polarization greater than 18 dB over a fiber length of $> 2.25\text{ m}$. An all-fiber oscillator structure test platform is built to achieve a laser output of 48.9 W at 1064 nm , and the slope efficiency is as high as 85.5% . The high laser performance of the PM fiber is verified, laying a solid foundation for the localization of high-performance PM fibers.

Key words laser optics; fiber optics; fiber laser oscillator; fiber measurements; ytterbium-doped polarization-maintaining fibers